

Diagnosis and Detection Fault in Induction Motor Fed by Three Multi level Inverter

Youcef Soufi ¹, Tahar Bahi ², Mohamed Faouzi Harkat ³, and Issam Atoui ²

¹ Department of Electrical Engineering, Tébessa University, Algeria
y_soufi@yahoo.fr

² Department of Electrical Engineering, Annaba University, Algeria
tbahi@hotmail.com , atoui_article@yahoo.fr

³ Department of Electronic Engineering, Annaba University, Algeria
mharkat@univ-annaba.org

Abstract. *The early detection for motor deterioration can increase plant availability and safety in an economical way. Many publications have investigated the detection and diagnosis of broken rotor bars in electrical machines supplied directly on line or supplied by pulse width modulation (PWM) voltage source inverter. However, much fewer research results have been published when the induction motor is fed by multilevel inverter voltage source for the applications requiring high power. The multilevel inverter drives become a solution not only for higher power applications and traction drives but also for the renewable energy. In this paper, we present a technical method based on spectral analysis of stator currents for detection of broken rotor bars in induction motor when it is fed from three level voltage inverter. Using more sophisticated models of the type of multi-circuit windings meshes adopted for the faults. The obtained simulation results show clearly that motor current signature analysis can effectively detect and locate fault in squirrel cage motor feed by the three level voltage inverter.*

Keywords. *Fault diagnosis, multilevel inverter, induction motor, broken rotor bar.*

1. Introduction

In the last decades, the induction motor has become the widest motor for industry. This is mainly due to its low cost, reasonably small size, ruggedness, low maintenance, and operation with an easily available power supply. On the other hand, the spreading of power electronics and the development of specific control techniques have made the induction machine a good solution for very different kind of applications [1]. Substantial operational costs in industrial plants are related to maintenance. In many cases, there is a lack of factual data to determine the real need for repair or

maintenance of machinery, equipment and industrial plant systems. Induction motors can be found in almost all types of applications. It is prone to many problems, such as broken bars, eccentricities, shorted windings and bearing defects. These problems are usually detected when the machine is broken, and sometimes, after irreversible damage. Condition monitoring can significantly reduce maintenance costs and the risk of unexpected failures through the early detection of potentials risks. However, there must be an accurate means of condition assessment and fault diagnosis [2]. The area of system maintenance can not realize its full potential if it is only limited to preventive approaches. In general, fault diagnosis of induction motors has concentrated on sensing failures in the stator, the rotor, bearings, and especially in the motor loads. Even though mechanical sensing techniques based on thermal and vibration monitoring have been widely utilized, most of the recent research has been directed toward electrical sensing with emphasis on analyzing the motor stator current [3]. On line fault diagnostics of induction motors are very important to ensure safe operation, timely maintenance, increased operation reliability, and preventive rescue. In recent years, intensive research efforts have been focused on developing new techniques for monitoring and diagnosing electrical machines. Unfortunately, most of these works consider the diagnosis of a machine powered directly from the network. However, in the industrial reality, the use of diagnostic machine when fed by an inverter is interesting. Thus, the method presented in this paper seems one of the powerful methods for diagnosing motor faults and have recently been successfully applied to diagnosis the rotor faults of large induction motor used in the industrial field and it becomes the standard of online motor diagnosis. The main advantage of this technique is its ability to extract automatically the characteristic frequencies relative to the different machine operating modes [4] [5]. So, we are interested, in this paper the use of spectral analysis of stator current for detection of broken rotor bars in squirrel cage motor fed by the three level voltage inverter. The obtained results show clearly that motor current signature analysis can effectively detect abnormal operating conditions in induction motor applications and the possibility of extracting signatures to detect and locate fault.

2. System and Mathematical Model

The three level voltage inverter is a new conversion structure used for supplying high power motor. Industry has begun to demand higher power ratings, and multi-level inverter drives have become a solution for high-power applications in recent years. A multilevel inverter not only achieves high-power ratings but also enables the use of renewable energy sources. Renewable energy sources such as photovoltaic, wind, and fuel cells can be easily interfaced to a multilevel converter system for high-power applications [6]. There are several structures of the three level inverter [7]. In this paper, we present the three-level neutral point clamp inverter supplying a squirrel induction motor. The figure 1 shows the configuration of the three level inverter. It consists of twelve switches bicommandables and bidirectional current and six uni-

directional current switches connected to the midpoint of the two sources, allowing access to p

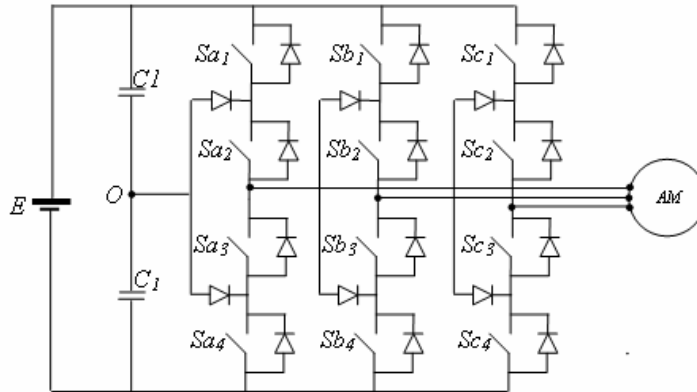


Fig. 1. Configuration of three level inverte

For different control strategies, the voltage issued from this type of inverter rate lower harmonics than which it corresponds to the voltages supplied by a conventional structure of two-level inverter. At the end of defining different configurations of three-phase inverter at three levels, we consider the view the symmetry of three level modeling inverter. We consider only one arm as show in figure. 2.

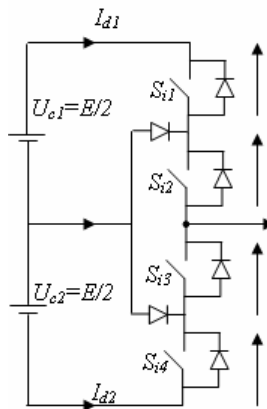


Fig. 2. Structure of one arm of the inverter

Table1 shows the switching states and output voltage. By turning on two switches of upper (S_1, S_2), lower (S_3, S_4) or middle (S_2, S_3), the output voltage can be clamped to the positive (P state), negative (N state) or zero potential (0 state), respectively. Since three kinds of switching state exist in each phase, the three-level inverter has twenty seven $27(3^3)$ switching states [7].

Table. 1. Switching voltage and output voltage

Switching states	S_1	S_2	S_3	S_4	V_n
P	ON	ON	OFF	OFF	+ E/2
0	OFF	ON	ON	OFF	0
N	OFF	OFF	ON	ON	- E/2

3. Model of Squirrel Cage Induction Machine

The rotor of the squirrel cage motor consists of q isolated bars, uniformly distributed over the surface of the rotor. Each bar of the rotor cage is modeled by a resistance R_b [8] in series with a leakage inductance L_b and each portion of the ring of short circuit with a resistance R_e in series with a leakage inductance L_e , as shown in figure 3.

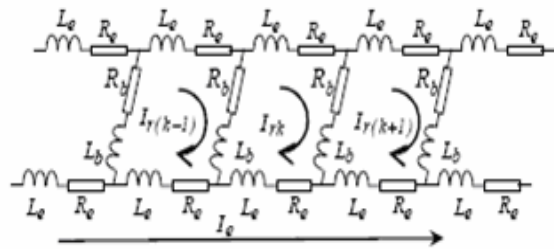


Fig. 3. Rotor mesh circuit

With application of Kirchoff's laws on the circuit described on figure 3, the form of $[R_r]$ rotor resistance matrix and $[L_r]$ rotor inductance matrix can be easily derived. It is also apparent that the calculation of all magnetizing and mutual inductances as defined in the previous equations is the key to successful simulation of the squirrel cage induction machine.

The application of Kirchoff's law on a grid gives us:

$$2.(R_b + R_e)j_k - R_b.j_{k+1} - R_b.j_{k-1} - R_e.j_e = 0 \tag{1}$$

$$\frac{d}{dt} [(L_{rkrk} + 2(L_b + L_e)j_k + (L_{rkrk1} - L_b)j_{k+1} + (L_{rkrk1} - L_b)j_{k-1} + \dots - L_e.j_e + L_{rks1}j_{s1} + \dots + L_{rksm}j_{sm}] = 0 \tag{2}$$

For the stator, it is assumed that it is composed of three phases each consisting of coils placed in series, regularly distributed in slots on all of its bore. We'll develop an analytical model of induction machine from the general equations; we calculate different inductance of the machine. For this purpose, it suffices to consider the me-

chanical angle (θ_{sisj}) difference between the i and j stator phases in the calculation of flux. The three phase squirrel cage induction machine equations with q rotor bars can be written as follow:

$$[V_s] = [R_s][I_s] + \frac{d\Phi_s}{dt} \quad (3)$$

With,

$$[V_s] = [V_{sa} \quad V_{sb} \quad V_{sc}]^t \quad (4)$$

$$[I_s] = [I_{sa} \quad I_{sb} \quad I_{sc}]^t \quad (5)$$

$$[\Phi_s] = [L_s][I_s] + [L_{sr}][I_r] \quad (6)$$

And,

$$[V_r] = [R_r][I_r] + \frac{d\Phi_r}{dt} \quad (7)$$

With,

$$[V_r] = [0 \quad 0 \quad 0 \quad \dots \quad 0]_{1 \times q+1}^t \quad (8)$$

$$[I_r] = [I_{r1} \quad I_{r2} \quad I_{r3} \quad \dots \quad I_{rq} \quad I_e]^t \quad (9)$$

$$[\Phi_r] = [L_{sr}]^t [I_s] + [L_r][I_r] \quad (10)$$

The resistance and inductance matrix are respectively represented by the following general form:

$$[F] = \begin{bmatrix} [F_s] & [F_{sr}] & [0] \\ [F_{sr}] & [F_r] & [-F_e] \\ [0] & [-F_e] & [q.F_e] \end{bmatrix} \quad (11)$$

With:

$F \equiv R$, resistance matrix

$F \equiv L$, inductance matrix

$F_{rs} \equiv F_{sr} = 0$, for considered resistance matrix

The matrix of inductances of stator phases expressed by the relationship (12) is of the order (m, m) with $m=3$:

$$[L_s]_{3 \times 3} = \begin{bmatrix} L_{saa} & L_{sab} & L_{sac} \\ L_{sba} & L_{sbb} & L_{sbc} \\ L_{sca} & L_{cb} & L_{scc} \end{bmatrix} \quad (12)$$

With:

L_{sii} if ($i=j$): the proper inductance of the phase i ;

L_{sij} if ($i \neq j$): mutual inductance between i and j stators phase

The matrix of rotor inductance is of the order $(q+1, q+1)$.

$$[L_r] = \begin{bmatrix} L_{r11} & L_{r12} & \cdots & \cdots & L_{r1q} & L_e \\ L_{r21} & L_{r2p} & \cdots & \cdots & L_{r2q} & L_e \\ \vdots & \vdots & \vdots & \vdots & \vdots & \vdots \\ \vdots & \vdots & \vdots & \vdots & \vdots & \vdots \\ L_{rq1} & L_{rq2} & \cdots & \cdots & L_{rqq} & L_e \\ L_e & L_e & \cdots & \cdots & L_e & qL_e \end{bmatrix} \quad (13)$$

The mutual inductance matrix between stator phases and rotor mesh is of the order (m, N_b) :

$$[L_{sr}] = \begin{bmatrix} L_{s1r1} & L_{s1r2} & \cdots & \cdots & L_{s1r_q} \\ L_{s2r1} & L_{s2r2} & \cdots & \cdots & L_{s2r_q} \\ L_{s3r1} & L_{s3r2} & \cdots & \cdots & L_{s3r_q} \end{bmatrix} \quad (14)$$

The rotor resistance matrix is:

$$[R_r] = \begin{bmatrix} R & -R_b & 0 & \cdots & 0 & -R_b & R_e \\ -R_b & R & -R_b & 0 & \cdots & 0 & R_e \\ \ddots & \ddots & \ddots & \ddots & \ddots & \ddots & \vdots \\ \ddots & \ddots & \ddots & \ddots & \ddots & \ddots & \vdots \\ \ddots & \ddots & \ddots & \ddots & \ddots & \ddots & \vdots \\ -R_b & 0 & \cdots & 0 & -R_b & R & R_e \\ R_e & R_e & \cdots & \cdots & \cdots & R_e & qR_e \end{bmatrix} \quad (15)$$

With:

$$[L_{rs}] = [L_{sr}]^T \quad \text{and} \quad R = 2(R_b + R_e) \quad (16)$$

The model presented in equation (3) and (7) is resolved as follows:

$$[\dot{I}] = -[L]^{-1} [R + L] [I] + [L]^{-1} [V] \tag{17}$$

Where:

$$[I] = \begin{bmatrix} [I_s] \\ [I_r] \end{bmatrix}, \quad [V] = \begin{bmatrix} [V_s] \\ [V_r] \end{bmatrix} \tag{18}$$

Inductions can be calculated either by using the winding functions as did by [9], knowing that it requires a precise knowledge of the shape of the winding machine, or by using decomposition into Fourier series of induction gap of the machine. The presence of a broken bar in the cage rotor produces a geometric and electromagnetic asymmetry in the rotor circuit and induced currents are created in direct rotating field, another field is turning around.

These electrical equations must be added to the following mechanical equation:

$$J \frac{d\Omega}{dt} = T_e - T_l + f_v \cdot \Omega \tag{19}$$

The electromagnetic torque is calculated by using the basic principle of energy conversion, the torque developed by the machine T_e can be obtained by considering the change in co-energy (W_{co}) of the system produced by a small change in rotor position when the currents are held constantly [10] deriving the latter expression with respect to the position taken by the rotor towards the stator. The expression of electromagnetic torque is ultimately determined by the relationship below [11]:

$$T_e = \left[\frac{\partial W_{co}}{\partial \theta_r} \right]_{(i_{3s}, i_m = const)} \tag{20}$$

It follows that the electromagnetic torque can be expressed as:

$$T_e = [i_s]^t \frac{\partial [L_{sr}]}{\partial \theta_r} [i_r] \tag{21}$$

$$T_e = \frac{1}{2} \begin{bmatrix} [I_s] \\ [I_r] \end{bmatrix}^t \frac{d}{d\theta} \begin{bmatrix} [L_s] & [L_{sr}] \\ [L_{rs}] & [L_r] \end{bmatrix} \begin{bmatrix} [I_s] \\ [I_r] \end{bmatrix} \tag{22}$$

Where: $[L_s]$, $[L_r]$, $[L_{sr}]$ and $[L_{rs}]$, are respectively the matrix of proper and mutual inductances of stator and rotor windings.

3.1. Rotor faults

Figure 4 shows the circuit representation of a broken bar . In this case, it is apparent from the theory that all parameters related to the loop one (1) must change, while the equation remains the same except the equation related to the loop too (2) which is dropped. Inductances related to the faulty bar are recalculated when fault occurs. However, the equations related to loop 2 and n must be modified and the equation related to loop 1 is dropped. So, modifying the faulty bar resistance R_b with a higher value than the nominal [12].

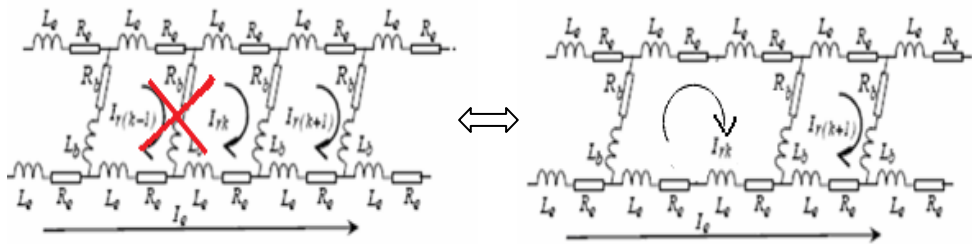


Fig. 4. Equivalent circuit for one broken bar

The modeling of a fracture of a bar or a ring segment (see figure 4) by increasing the value of its resistance so that the current crossing is the most close to zero in steady state. This is introduced in the matrix of resistances by the addition of the matrix of the rotor resistance $[R_r]$ with the default matrix $[R_f]$. In our study, the method of modeling by increasing the resistance of the broken bar, the value of this resistance is multiplied by a factor of $M = 10^3$.

$$[R_f] = \begin{bmatrix} 0 & 0 & 0 & \dots & 0 \\ \vdots & 0 & \dots & \dots & 0 \\ \vdots & R_{k,k} & R_{k,k+1} & 0 & \vdots \\ 0 & R_{k+1,k} & R_{k+1,k+1} & \vdots & \vdots \\ 0 & \dots & \dots & 0 & 0 \end{bmatrix} \quad (23)$$

With:

$$R_{k,k} = R_{k+1,k+1} = (M + 1).R_b + 2.R_e; \quad R_{k+1,k} = R_{k,k+1} = (-M).R_b;$$

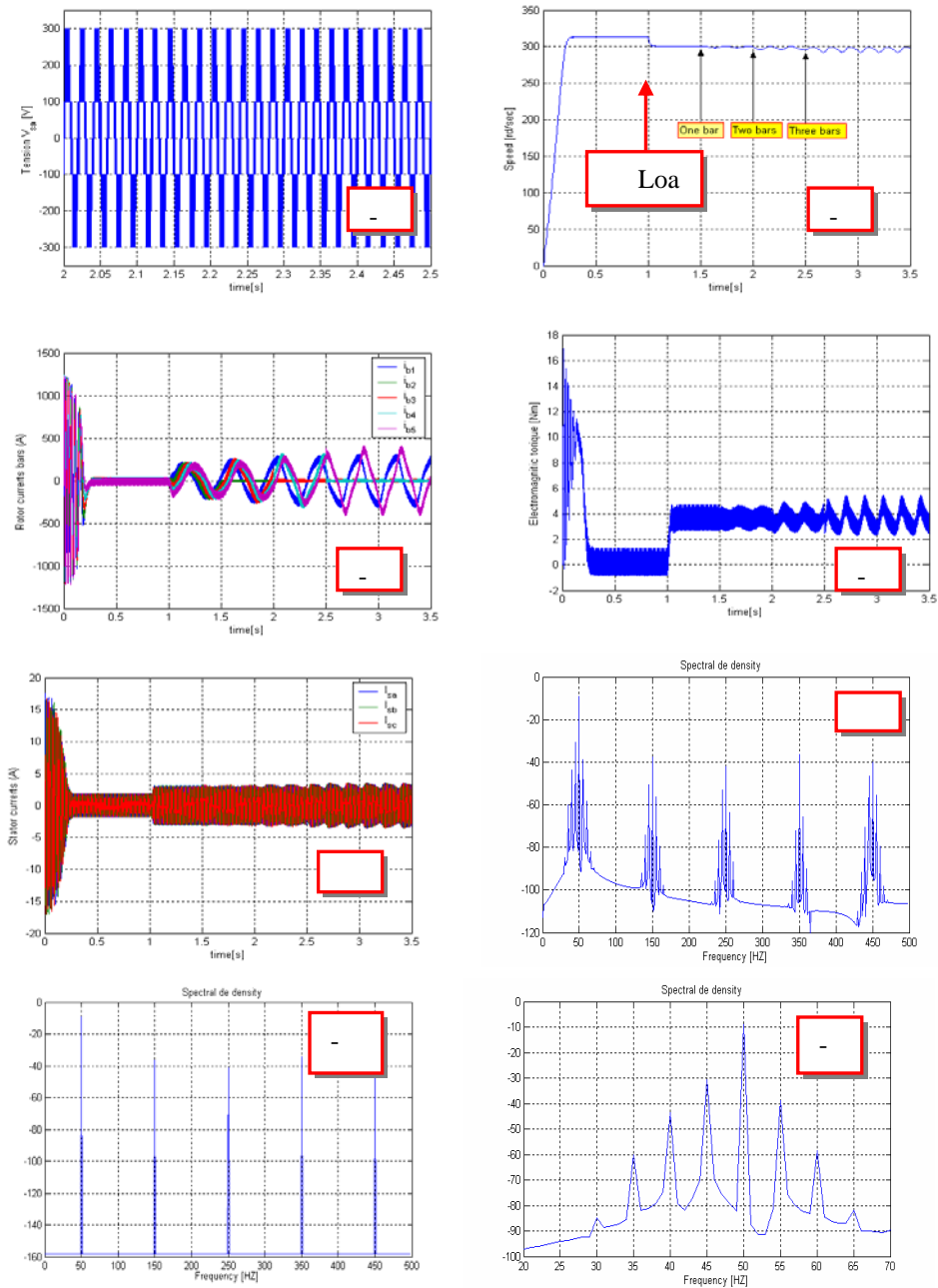


Fig. 5. Simulation Results

4. Simulation Results

Figure 5a presents a zoom on the output voltage of the inverter feeding the motor. We see clearly the three levels of voltage. Figures 5b, 5c, and 5d show respectively the behaviors of the speed of currents of the four rotor bars and the electromagnetic torque. We notice that for every break, previous oscillations magnitudes increases. So, with this result, we can conclude that if we can not detect the fracture in its early appearances, the current flowing through the adjacent cross bar (see fig. 5c) resulting in its heating and consequently its fracture. Following this finding, it is advisable and essential to detect the break so early in order to protect the functionality of the machine and avoid its deactivation. Figure 5d shows that the first break at time 1.5 seconds during which crossed the bar is zero and therefore the amplitude of the currents of adjacent bars increases. This phenomenon is seen when one of the bars is broken. It is important to note that the effect of breaks appears directly on the stator currents (see fig. 5e) with the envelope that is formed with undulations. Therefore, since this signal is easily measured, it is worthwhile to analyze in order to detect defects. First we apply spectral analysis on the first part of the signal (healthy case) and we obtained the result of Figure 5g. We note the appearance of frequencies of the order k.fs, (50, 100, 150, 200 ...) notably including fundamental 50 Hz, others are multiples. These are the use of voltage inverter. Furthermore, the analysis on the portion representing the default provides the spectral representation of Figure 5f and its zoom in figure 5h. We notice that with much more frequencies, that accounts healthy case other frequencies appear. These are the signatures of defects breaks of barres. However, we recall that in case of motor powered directly by a pure sine wave, only one harmonic appear. On the contrary, when it is fed by the three level inverter, we notice the appearance of frequencies: 35, 40, 45, 50, 55, 60 and 65 which appear

5. Conclusion

The good knowledge and information about the fault mode behaviour of induction motor fed by a three level source inverter is necessary to improve system design and protection. This paper presents the simulation of induction machines fed by a three multilevel source inverter with broken rotor bars faults and the fault signature analysis of stator current. The electrical model of induction motor under faulty condition is given and the start up is simulated. The features of stator current of healthy conditions of a three-phase induction motor are compared with that of the faulty conditions with three broken rotor bars. The results show that motor current signature analysis can effectively detect broken rotor bars and detect abnormal operating conditions in induction motor applications for diagnosis and detection fault systems. The technique used allows detection of faults in induction machine and the obtained simulation results show clearly the efficacy of its analysis and the impact of such default on the current spectrum and the model for diagnosis.

References

1. Bracale, A., Carpinelli, G., Piegari, L., Tricoli, P.: A High Resolution Method for On Line, Diagnosis of Induction Motors Faults. pp: 994-998, IEEE 2007
2. Sergio .P.S., Alfredo J.F.C: A comparison between Hybrid and no-hybrid classifiers in diagnosis of induction motor faults. 11th IEEE International Conference on Computational Science and Engineering, 2008.
3. Eltabach, M., Hamdan', H.: Induction motor fault detection by spectral principal components analysis of the supply currents. IEEE International Symposium on Industrial Electronics (ISIE 2009), Seoul Olympic Parktel, Seoul, pp: 1111-1116; Korea July 5-8; 2009
4. Jung, J.H., Lee, J.J., and Kwon, B. H.: Online Diagnosis of Induction Motors Using MCSA. IEEE Transactions on Industrial Electronics, vol. 53, N° 6, pp 1842- 1852, December 2006.
5. Ye, Z., Wu, B.: Classification Induction Motor Mechanical Fault Simulation and Stator Current Signature Analysis, pp: 789-794; IEEE 2000.
6. Khomfoi, S., Tolbert, L.M.: Fault Diagnosis and Reconfiguration for Multilevel Inverter Drive Using AI-Based Techniques. IEEE Transactions on Industrial Electronics, vol. 54, N°. 6, pp: 2954- 2967, December 2007.
7. Son, H.I., Kim, T.J., Kang, D.W, Hyun, D.S.: Fault Diagnosis and Neutral Point Voltage Control When The 3-Level Inverter Faults Occur .35th Annual IEEE Power Electronics Specialists Conference, pp: 4558-4563, Aachen, Germany, 2004.
8. S. Nandi, S. Ahmed, and H.A. Toliyat.: Detection of rotor slot and other eccentricity related harmonics in a three phase induction motor with different rotor cages. IEEE Transactions on Energy Conversion, vol. 16, N° 3, pp. 253–260, Sept. 2001.
9. Khezzar, A., Hadjami, M., N. Bessous, Maamar , Mek., Razik , H.: Accurate Modeling of Cage Induction Machine with Analytical Evaluation of Inductances. IEEE , pp.1112-1117, 2008.
10. Rouaibia, R., Bahi ,T. and Fisli , M.: Detection of Broken and ring rotor Barres in induction motor fed by an voltage source inverter . 6 th conferences on Electrical Engineering EMP Alger, 2009.
11. Ayhan, B., Chow, M. Y. and Song, M.H. : Multiple Signature Processing-Based Fault Detection Schemes for Broken Rotor Bar in Induction Motors. IEEE Transactions on Energy Conversion, Vol. 20, N°. 2, June 2005.

1083 IJ-STA, Volume 3, N°2, December, 2009.

12. Devanneaux, V., Kabbaj, H., Daques, B., and Faucher J.: an accurate Model of squirrel Cage Induction machines under rotor faults. IEEE, pp: 384-387, sept 2009.